

Possible multi-gap superconductivity in BiS₂-based layered superconductor Bi₄O₄S₃

P. K. Biswas,^{1,*} A. Amato,¹ C. Baines,¹ R. Khasanov,¹
H. Luetkens,¹ Hechang Lei,² C. Petrovic,² and E. Morenzoni^{1,†}

¹*Laboratory for Muon Spin Spectroscopy, Paul Scherrer Institute, CH-5232 Villigen PSI, Switzerland*

²*Condensed Matter Physics and Materials Science Department,
Brookhaven National Laboratory, Upton, New York 11973-5000, USA*

The magnetic penetration depth λ as a function of temperature in Bi₄O₄S₃ was studied using muon-spin-spectroscopy measurements. The dependence of λ^{-2} on temperature suggests the existence of two *s*-wave type energy gaps with the zero-temperature values of 1.117(3) and 0.16(1) meV for the large and small gaps, respectively. The presence of two superconducting energy gaps are consistent with two bands crossing the Fermi surface, as suggested by band structure calculation. This implies that like many Fe-based layered superconductors, Bi₄O₄S₃ is a multi-gap superconductor with fully developed energy gaps. The value of $\lambda(T)$ at $T = 0$ K is estimated to be $\lambda(0) = 819(1)$ nm.

PACS numbers: 74.25.F-, 74.25.Ha, 76.75.+i

In recent years, scientists have witnessed a growing interest in superconductivity within layered crystal structure compounds. The recent discovery of superconductivity in the BiS₂-based compound Bi₄O₄S₃ [1] with a transition temperature (T_c) of ≈ 4.5 K has again triggered an enormous research interest in layered superconductors. Exotic superconductivity with higher T_c and/or with unconventional pairing mechanism has often been found in materials with a layered crystal structure. In this context, the most familiar examples are the high- T_c cuprates and Fe-based superconductors, where the corresponding CuO₂ or Fe₂An₂ (An = P, As, Se, Te) layer plays an important role in determining the superconducting properties [2–4]. Similarly, the BiS₂ layer is believed to be the basic building block for inducing superconductivity in Bi₄O₄S₃ and it is also expected that the doping mechanism resembles that of cuprates and Fe-based superconductors. This argument is supported by the discovery of other BiS₂-based superconductors ReO_{1-x}F_xBiS₂ (Re = La, Ce, Pr, and Nd) with T_c values of 10.6, 3.0, 5.5, and 5.6 K, respectively [5–7, 9].

Up to now, only very few theoretical and experimental studies have been performed on Bi₄O₄S₃. The parent phase (Bi₆O₈S₅) is a band insulator which becomes superconducting after electron doping [1]. A first principles band structure calculation indicates that the superconductivity in Bi₄O₄S₃ originates from two Bi 6*p* orbitals, as they intersect the Fermi surface [10]. Transport measurements under pressure reveal that T_c of Bi₄O₄S₃ decreases monotonously without distinct change of the normal state metallic behavior [11]. Hall coefficient and magnetoresistance measurements suggest exotic multi-band features in Bi₄O₄S₃ [12]. Recent measurements of the temperature dependence of the magnetic penetration depth λ using the tunnel diode oscillator technique [13] indicate a conventional *s*-wave type superconductivity in Bi₄O₄S₃. However, the tunnel diode data were collected only down to 1.6 K and hence remain elusive in deter-

mining the true symmetry of the superconducting order parameter in Bi₄O₄S₃. To understand the microscopic pairing mechanism responsible for superconductivity in Bi₄O₄S₃, a detailed knowledge of the superconducting order parameter over the full temperature range is therefore very important.

In this Rapid Communication, we report on the results of muon-spin rotation and relaxation (μ SR) studies of the magnetic penetration depth as a function of temperature and on the symmetry of the superconducting gap in the Bi₄O₄S₃ superconductor. Our results indicate possible multi-gap superconductivity in Bi₄O₄S₃. The observed $\lambda^{-2}(T)$ is found to be well described by a two-gap *s*-wave model, as seen in many layered Fe-based superconductors. The gap values at absolute zero are $\Delta_1(0) = 1.117(3)$, $\Delta_2(0) = 0.16(1)$ meV. The corresponding gap to T_c ratios are $\Delta_1(0)/k_B T_c = 2.96(1)$ and $\Delta_2(0)/k_B T_c = 0.43(1)$. These values are close to those obtained for various Fe-based superconductors. We obtain the penetration depth, $\lambda(0) = 819(1)$ nm.

Polycrystalline samples of Bi₄O₄S₃ were prepared by a solid state reaction method [1]. Sample characterization measurements were performed at the Brookhaven National Laboratory, USA. Transport measurements at different applied fields were performed at the Paul Scherrer Institute (PSI), Villigen, Switzerland. Zero-field (ZF) and transverse-field (TF) μ SR experiments were carried out on the DOLLY and LTF μ SR instruments, located respectively at the π E1 and π M3 beamlines at the PSI. The sample was in the form of a pressed pellet and mounted on a copper fork shaped sample holder in DOLLY and on a silver plate in LTF instruments. The sample was cooled from above T_c to base temperature at $H = 0$ during ZF- μ SR experiments and in a field of 300 Oe in TF- μ SR experiments. The typical counting statistics were ~ 20 million muon decays per data point. The ZF and TF μ SR data were analyzed by using the free software package MUSRFIT [8].

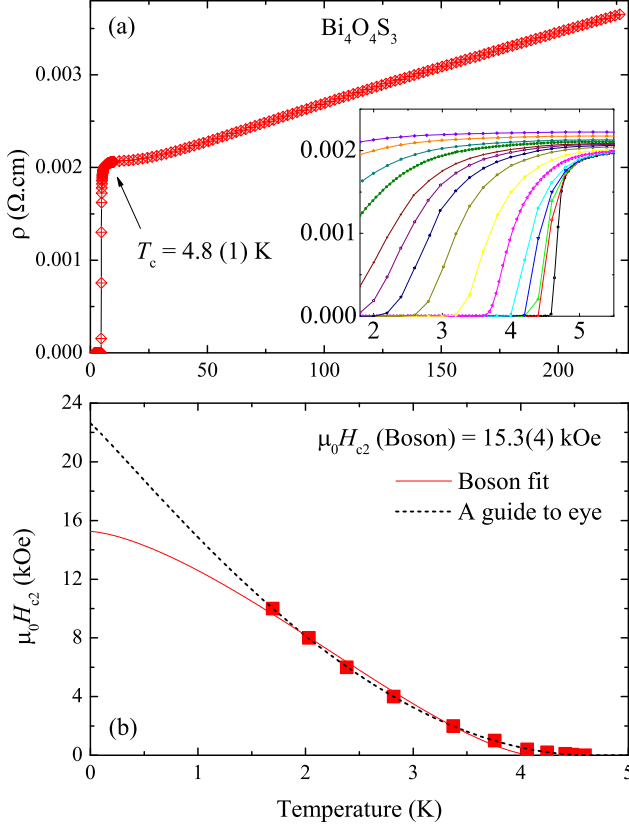


FIG. 1: (Color online) (a) Temperature dependence of the ac resistivity of $\text{Bi}_4\text{O}_4\text{S}_3$. Inset shows the temperature variation of the resistivity in a set of magnetic fields of 0, 0.05, 0.1, 0.2, 0.4, 1, 2, 4, 6, 8, 10, 15, 20, 30, and 40 kOe. (b) Temperature dependence of the upper critical field of $\text{Bi}_4\text{O}_4\text{S}_3$. The solid line is a fit to the data using an expression for charged boson. The dotted line is simply a guide to the eye.

The ac resistivity of $\text{Bi}_4\text{O}_4\text{S}_3$ was measured as a function of temperature using a standard four-probe method in a Physical Property Measurement System (PPMS). Figure 1 (a) shows the temperature dependence of the resistivity, $\rho(T)$. A metallic like behavior is observed between 5 K to 220 K with a relatively high residual resistivity value of 2 mΩ.cm and transition to the superconducting state with a T_c (onset) $\simeq 4.8(1)$ K. The inset shows the temperature variation of the resistivity in a set of magnetic fields from 0 to 40 kOe. $\rho(T)$ exhibits positive magnetoresistance (MR) in the normal state (just above T_c). At 6 K, the value of MR increases by 10.6 % for an applied magnetic field of 40 kOe. The temperature dependence of the upper critical field, H_{c2} , of $\text{Bi}_4\text{O}_4\text{S}_3$, shown in Fig. 1 (b), was determined from the resistive transitions, defined by a 90 % drop of the normal state resistivity values, determined just above T_c . The $H_{c2}(T)$ curve shows a positive curvature close to T_c and is linear thereafter. A similar behavior has also been observed in polycrystalline borocarbides [14], MgB_2 [15, 16],

$\text{Nb}_{0.18}\text{Re}_{0.82}$ [17], and Re_3W [18] and is considered as a signature of multi-gap superconductivity. A conventional Werthamer-Helfand-Hohenberg model can not describe $H_{c2}(T)$ of $\text{Bi}_4\text{O}_4\text{S}_3$. However, to estimate H_{c2} at absolute zero, a fit to the $H_{c2}(T)$ data was made using the $H_{c2}(T)$ expression for charged bosons [19],

$$H_{c2}(T) = H_{c2}(0) \left\{ 1 - \left(\frac{T}{T_c} \right)^{3/2} \right\}^{3/2}, \quad (1)$$

The fit yields $\mu_0 H_{c2}(0) = 24(1)$ kOe which implies a Ginzburg coherence length $\xi \approx 12$ nm. To get a better estimation of $H_{c2}(T)$ close to T_c , an empirical interpolation (shown as a dotted line in Fig. 1 (b)) was later used for calculating the temperature dependence of the penetration depth of $\text{Bi}_4\text{O}_4\text{S}_3$.

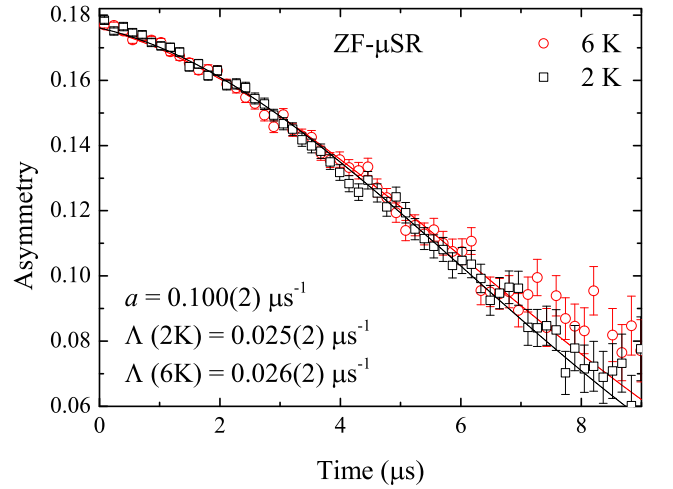


FIG. 2: (Color online) ZF- μ SR time spectra collected at 2 K and 6 K for $\text{Bi}_4\text{O}_4\text{S}_3$. The solid lines are the fits to the data using the Eq. 2, described in the text.

ZF- μ SR measurements were performed to look for any unusual temperature-dependent relaxation processes, which may be associated with the onset of superconductivity. Figure 2 shows the ZF- μ SR time spectra of $\text{Bi}_4\text{O}_4\text{S}_3$, collected below (at 2 K) and above (at 6 K) T_c . Practically, no difference between the two data sets is observable. This implies the absence of magnetic anomaly in the superconducting ground state of $\text{Bi}_4\text{O}_4\text{S}_3$. ZF- μ SR data can be described using a Kubo-Toyabe relaxation function [20] multiplied by an exponential decay function,

$$A(t) = A(0) \left\{ \frac{1}{3} + \frac{2}{3} (1 - a^2 t^2) \exp \left(-\frac{a^2 t^2}{2} \right) \right\} \exp(-\Lambda t), \quad (2)$$

where $A(0)$ is the initial asymmetry, and a and Λ are the muon spin relaxation rates. In the fit, a was kept as a common parameter for both set of data. The fits yield,

$a = 0.100(2) \mu\text{s}^{-1}$, $\Lambda(2\text{K}) = 0.025(2) \mu\text{s}^{-1}$, and $\Lambda(6\text{K}) = 0.026(2) \mu\text{s}^{-1}$. The value of a extracted from the fits reflects the presence of random local fields arising from the nuclear moments within $\text{Bi}_4\text{O}_4\text{S}_3$. The nearly equal values of Λ are consistent with the presence of diluted and randomly oriented electronic moments probably arising from impurities and are temperature independent.

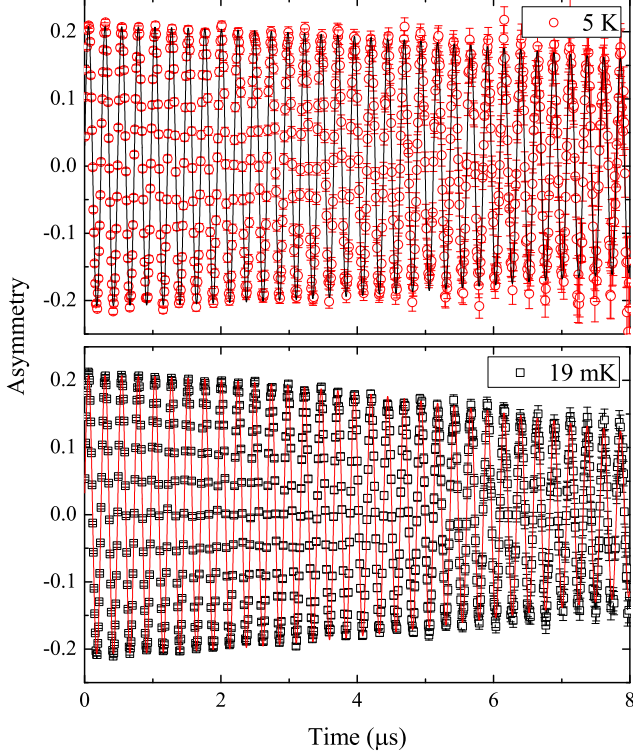


FIG. 3: (Color online) TF- μSR time spectra of $\text{Bi}_4\text{O}_4\text{S}_3$ collected at 19 mK and 5 K in a transverse field of 300 Oe. The solid lines are the fits to the data using the Eq. 3, described in the text.

Figure 3 shows the TF- μSR time spectra of $\text{Bi}_4\text{O}_4\text{S}_3$, collected at 19 mK and 5 K in a transverse field of 300 Oe. At 5 K, the sample is in the normal state and the local field probed by the muons is the applied field slightly broadened by the nuclear moments contribution, which is responsible for the weak relaxation of the precession signal. By contrast, the data collected at 19 mK shows a more pronounced damping due to the inhomogeneous field distribution, generated by the formation of a vortex lattice in $\text{Bi}_4\text{O}_4\text{S}_3$. The TF- μSR time spectra were analyzed using Gaussian damped spin precession signal,

$$A^{TF}(t) = A(0) \exp(-\sigma^2 t^2 / 2) \cos(\gamma_\mu B_{\text{int}} t + \phi) + A_{\text{bg}}(0) \cos(\gamma_\mu B_{\text{bg}} t + \phi), \quad (3)$$

where $A(0)$ and $A_{\text{bg}}(0)$ are the initial asymmetries of the sample and background signals, $\gamma_\mu/2\pi = 135.5 \text{ MHz/T}$ is the muon gyromagnetic ratio [21], B_{int} and B_{bg} are

the internal and background magnetic fields, ϕ is the initial phase of the muon precession signal, and σ is the Gaussian muon spin relaxation rate. Here, we assume non-decay background signal as it mainly come from the silver sample holder where muon decay rate is negligible.

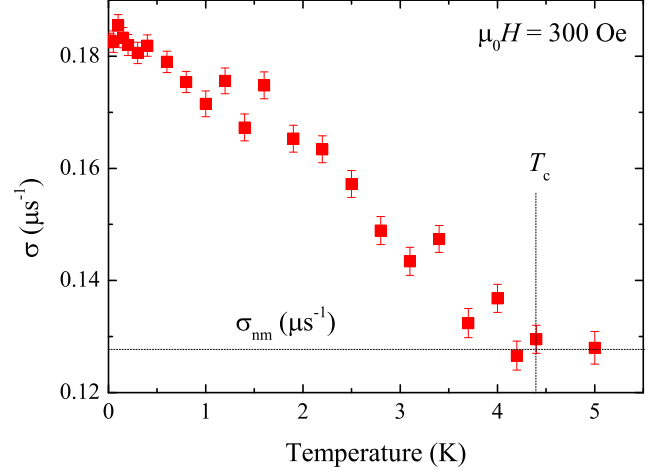


FIG. 4: (Color online) The temperature dependence of σ of $\text{Bi}_4\text{O}_4\text{S}_3$ for an applied field of 300 Oe. The dotted line parallel to the temperature axis showing the temperature independent value of σ_{nm} , the nuclear magnetic dipolar contribution to the σ .

Figure 4 shows the temperature dependence of σ for an applied field of 300 Oe. σ can be expressed as $\sigma = (\sigma_{\text{sc}}^2 + \sigma_{\text{nm}}^2)^{1/2}$, where σ_{sc} is the superconducting contribution to the relaxation rate due to the inhomogeneous field distribution arising from the vortex lattice and σ_{nm} is the nuclear magnetic dipolar contribution which is assumed to be temperature independent. Value of σ_{nm} is $0.128(1) \mu\text{s}^{-1}$.

For a superconductor with hexagonal vortex lattice, σ_{sc} is related to the penetration depth, λ by the Brandt equation [23], which is based on a Ginzburg-Landau treatment of the vortex state,

$$\sigma_{\text{sc}}(b) [\mu\text{s}^{-1}] = 4.854 \times 10^4 (1-b) [1 + 1.21(1-\sqrt{b})^3] \lambda^{-2} [\text{nm}^{-2}], \quad (4)$$

Here $b = B/B_{c2}$ is the reduced magnetic field and B is the applied field. Eq. 4 was used to calculate $\lambda^{-2}(T)$, which is proportional to the superfluid density. Figure 5 shows the temperature dependence of λ^{-2} for $\text{Bi}_4\text{O}_4\text{S}_3$. The fits to the $\lambda^{-2}(T)$ data of $\text{Bi}_4\text{O}_4\text{S}_3$ were then made with a single-gap and two-gap s -wave models using the following functional form [24, 25]:

$$\frac{\lambda^{-2}(T)}{\lambda^{-2}(0)} = \omega \frac{\lambda^{-2}(T, \Delta_1(0))}{\lambda^{-2}(0, \Delta_1(0))} + (1-\omega) \frac{\lambda^{-2}(T, \Delta_2(0))}{\lambda^{-2}(0, \Delta_2(0))}, \quad (5)$$

where $\lambda(0)$ is the value of the penetration depth at $T = 0 \text{ K}$, $\Delta_i(0)$ is the value of the i -th ($i = 1$ or 2)

superconducting gap at $T = 0$ K and ω is the weighting factor of the first gap.

Each component of Eq. 5 can be expressed within the local London approximation ($\lambda \gg \xi$) [26, 27] as

$$\frac{\lambda^{-2}(T, \Delta_i(0))}{\lambda^{-2}(0, \Delta_i(0))} = 1 + 2 \int_{\Delta_i(0)}^{\infty} \left(\frac{\partial f}{\partial E} \right) \frac{EdE}{\sqrt{E^2 - \Delta_i(T)^2}}, \quad (6)$$

where $f = [1 + \exp(E/k_B T)]^{-1}$ is the Fermi function, and $\Delta_i(T) = \Delta_i(0)\delta(T/T_c)$. The temperature dependence of the gap is approximated by the expression $\delta(T/T_c) = \tanh \left\{ 1.82 [1.018 (T_c/T - 1)]^{0.51} \right\}$ [24].

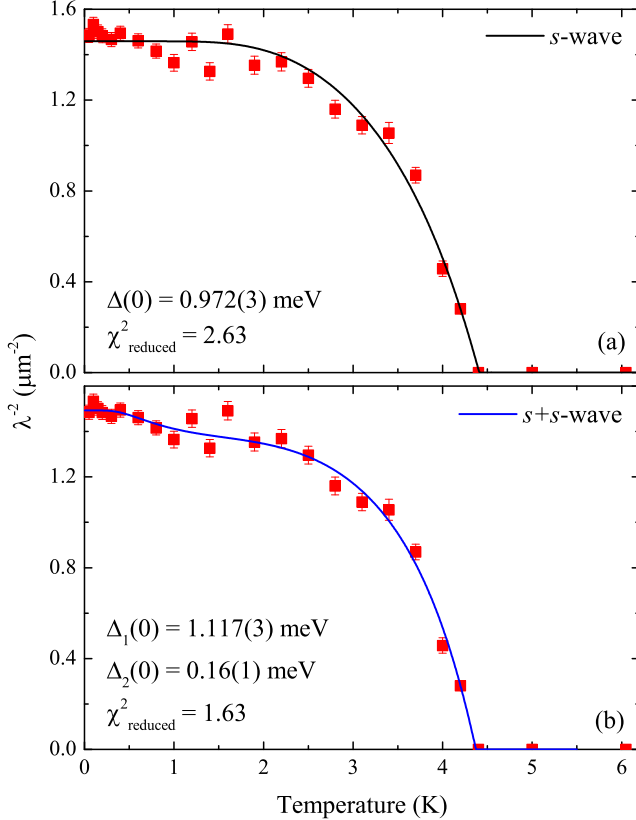


FIG. 5: (Color online) Temperature dependence of λ^{-2} for $\text{Bi}_4\text{O}_4\text{S}_3$. The curves are fits to the data using a (a) single-gap and (b) two-gap s -wave models.

The curves shown in Fig. 5 (a) and (b) are the fits to the $\lambda^{-2}(T)$ data of $\text{Bi}_4\text{O}_4\text{S}_3$ using a single-gap and two-gap s -wave models, respectively. Table I summarizes all the fitted parameters from the two different model fits. The two s -wave gap model gives a much lower χ^2_{reduced} value than a single gap model. Our results appear to rule out the single gap s -wave as a possible model for this system, as claimed in Ref. 13 and suggest that like many Fe-based layered superconductors [29–32], $\text{Bi}_4\text{O}_4\text{S}_3$ is also a multi-gap superconductor. For the two-gap s -

TABLE I: Fitted parameters of the fits to the $\lambda^{-2}(T)$ data of $\text{Bi}_4\text{O}_4\text{S}_3$ using different models.

Model	Gap value $\Delta(0)$ (meV)	Gap ratio $\Delta(0)/k_B T_c$	χ^2_{reduced}
s-wave	0.972(3)	2.56(1)	2.63
s+s-wave	1.117(3), 0.16(1) with $\omega = 0.89(1)$	2.96(1), 0.43(1)	1.63

wave model, we obtain $\lambda(0) = 819(1)$ nm, one of the highest among all other known superconductors.

In summary, resistivity and μSR measurements have been performed on superconducting $\text{Bi}_4\text{O}_4\text{S}_3$. Temperature dependence of the upper critical fields and also the absolute value, $H_{c2}(0) = 24(1)$ kOe were calculated from the resistivity measurements. The $H_{c2}(T)$ data shows a positive curvature close to T_c , which is a sign of multi-gap superconductivity in $\text{Bi}_4\text{O}_4\text{S}_3$. TF- μSR results show that the temperature dependence of λ^{-2} is compatible with a two-gap s -wave model with the zero-temperature gap values, $\Delta_1(0) = 1.117(3)$, $\Delta_2(0) = 0.16(1)$ meV and penetration depth, $\lambda(0) = 819(1)$ nm. It is worth mentioning that the presence of two superconducting gaps in $\text{Bi}_4\text{O}_4\text{S}_3$ found from the μSR study are consistent with two bands crossing the Fermi surface, as suggested by first principles band structure calculation in Ref. 10. Our results suggest that like many layered Fe-based superconductors, the superconducting energy gap in $\text{Bi}_4\text{O}_4\text{S}_3$ superconductor is fully developed and contains no nodes. Further study on high-quality single-crystal samples (once available) will shed more light on the true nature of the superconducting state [28].

The μSR experiments were performed at the Swiss Muon Source ($\text{S}\mu\text{S}$), Paul Scherrer Institute (PSI, Switzerland). Work at Brookhaven is supported by the Center for Emergent Superconductivity, an Energy Frontier Research Center funded by the DOE Office for Basic Energy Science (H.L. and C.P.). P.K.B. would like to acknowledge M. Medarde and R. Sibille for their assistance in transport measurements.

* Corresponding author: pabitra.biswas@psi.ch

† Corresponding author: elvezio.morenzoni@psi.ch

- [1] Y. Mizuguchi, H. Fujihisa, Y. Gotoh, K. Suzuki, H. Usui, K. Kuroki, S. Demura, Y. Takano, H. Izawa, and O. Miura, Phys. Rev. B **86**, 220510(R) (2012).
- [2] J.G. Bednorz, and K.A. Muller, Z. Physik B **64**, 189 (1986).
- [3] Y. Kamihara, T. Watanabe, M. Hirano, and H. Hosono, J. Am. Chem. Soc. **130**, 3296 (2008).
- [4] F.-C. Hsu, J.-Y. Luo, K.-W. Yeh, T.-K. Chen, T.-

- W. Huang, P.M. Wu, Y.-C. Lee, Y.-L. Huang, Y.-Y. Chu, D.-C. Yan, and M.-K. Wu, *Proc. Natl. Acad. Sci. USA* **105**, 14262 (2008).
- [5] Y. Mizuguchi, S. Demura, K. Deguchi, Y. Takano, H. Fujihisa, Y. Gotoh, H. Izawa, and O. Miura, *J. Phys. Soc. Jpn.* **81** 114725 (2012).
- [6] J. Xing, S. Li, X. Ding, H. Yang, and H.-H. Wen, *Phys. Rev. B* **86**, 214518 (2012).
- [7] R. Jha, A. Kumar, S.K. Singh, and V.P.S. Awana, *J. Sup. and Novel Mag.* **26**, 499 (2013).
- [8] A. Suter, and B.M. Wojek, *Physics Procedia* **30**, 69 (2012).
- [9] S. Demura, Y. Mizuguchi, K. Deguchi, H. Okazaki, H. Hara, T. Watanabe, S.J. Denholme, M. Fujioka, T. Ozaki, H. Fujihisa, Y. Gotoh, O. Miura, T. Yamaguchi, H. Takeya, and Y. Takano, *J. Phys. Soc. Jpn.* **82** 033708 (2013).
- [10] H. Usui, K. Suzuki, and K. Kuroki, *Phys. Rev. B* **86**, 220501(R) (2012).
- [11] H. Kotegawa, Y. Tomita, H. Tou, H. Izawa, Y. Mizuguchi, O. Miura, S. Demura, K. Deguchi, and Y. Takano, *J. Phys. Soc. Jpn.* **81** 103702 (2012).
- [12] S. Li, H. Yang, J. Tao, X. Ding, and H.-H. Wen, *Sci. China-Phys. Mech. Astron.* **56**, 2019 (2013).
- [13] Shruti, P. Srivastava, and S. Patnaik, arXiv:1305.6913.
- [14] S.V. Shulga, S.-L. Drechsler, G. Fuchs, K.-H. Müller, K. Winzer, M. Heinecke, and K. Krug, *Phys. Rev. Lett.* **80**, 1730 (1998).
- [15] I. Shigeta, T. Abiru, K. Abe, A. Nishida, and Y. Matsumoto, *Physica C* **392-396**, 359 (2003).
- [16] Y. Takano, H. Takeya, H. Fujii, H. Kumakura, T. Hatano, K. Togano, H. Kito, and H. Ihara, *Appl. Phys. Lett.* **78**, 2914 (2001).
- [17] A.B. Karki, Y.M. Xiong, N. Haldolaarachchige, S. Stadler, I. Vekhter, P.W. Adams, D.P. Young, W.A. Phelan, and J.Y. Chan, *Phys. Rev. B* **83**, 144525 (2011).
- [18] P.K. Biswas, M.R. Lees, A.D. Hillier, R.I. Smith, W.G. Marshall, and D.McK. Paul, *Phys. Rev. B* **84**, 184529 (2011).
- [19] R. Micnas, J. Ranninger, and S. Robaszkiewicz, *Rev. Mod. Phys.* **62**, 113 (1990).
- [20] R. Kubo, *Hyperfine Interact.* **8**, 731 (1981).
- [21] J.E. Sonier, J.H. Brewer, and R.F. Kiefl, *Rev. Mod. Phys.* **72**, 769 (2000).
- [22] E.H. Brandt, *Phys. Rev. B* **37**, 2349 (1988).
- [23] E.H. Brandt, *Phys. Rev. B* **68**, 054506 (2003).
- [24] A. Carrington, and F. Manzano, *Physica C* **385**, 205 (2003).
- [25] H. Padamsee, and J.E. Neighbor, and C.A. Shiffman, *J. Low Temp. Phys.* **12**, 387 (1973).
- [26] M. Tinkham, *Introduction to Superconductivity* (McGraw-Hill, New York, 1975).
- [27] R. Prozorov, and R.W. Giannetta, *Supercond. Sci. Technol.* **19**, R41 (2006).
- [28] J.E. Sonier, J.H. Brewer, R.F. Kiefl, G.D. Morris, R.I. Miller, D.A. Bonn, J. Chakhalian, R.H. Heffner, W.N. Hardy, and R. Liang, *Phys. Rev. Lett.* **83**, 4156 (1999), and the references therein.
- [29] R. Khasanov, K. Conder, E. Pomjakushina, A. Amato, C. Baines, Z. Bukowski, J. Karpinski, S. Katrych, H.-H. Klauss, H. Luetkens, A. Shengelaya, N.D. Zhigadlo, *Phys. Rev. B* **78**, 220510(R) (2008).
- [30] P.K. Biswas, G. Balakrishnan, D.McK. Paul, C.V. Tomy, M.R. Lees, A.D. Hillier, *Phys. Rev. B* **81**, 092510 (2010).
- [31] P.K. Biswas, A. Krzton-Maziopa, R. Khasanov, H. Luetkens, E. Pomjakushina, K. Conder, and A. Amato, *Phys. Rev. Lett.* **110**, 137003 (2013).
- [32] J. Paglione, and R.L. Greene, *Nat. Phys.* **6**, 645 (2010).